Time-Resolved EPR, Fluorescence, and Transient Absorption Studies on Phthalocyaninatosilicon Covalently Linked to One or Two TEMPO Radicals

Kazuyuki Ishii,[†] Yoshiharu Hirose,[†] Hiroshi Fujitsuka,[‡] Osamu Ito,[‡] and Nagao Kobayashi*,[†]

Contribution from the Department of Chemistry, Graduate School of Science, Tohoku University, Sendai 980-8578, Japan, and Institute for Chemical Reaction Science, Tohoku University, Sendai 980-8577, Japan

Received July 25, 2000

Abstract: The photophysical properties of tetra-*tert*-butylphthalocyaninatosilicon (SiPc) covalently linked to one or two 2,2,6,6-tetramethyl-1-piperidinyloxy (TEMPO) radicals (R1, R2) have been studied by fluorescence, transient absorption, and time-resolved electron paramagnetic resonance (TREPR) spectroscopies. It is found that the fluorescence quantum yields and lifetimes of R1 and R2 decrease compared with those of (dihydroxy)-SiPc ((dihydroxy)SiPc = 6.8 ns, R1 = 4.7 ns and 42 ps, and R2 = 4.7 ns and <30 ps). Transient absorption measurements indicate that the lifetime of the excited triplet SiPc is markedly dependent on the number of linking TEMPO radicals ((dihydroxy)SiPc = 500 μs, R1 = 7.6 μs, and R2 = 3.7 μs). These short lifetimes of R1 and R2 in the excited states are explained as a result of the interaction with TEMPO changing the ISC between the singlet and triplet states to spin-allowed transitions. Quantitative TREPR investigations have been carried out for the radical-quartet pair mechanism of R1 and the photoinduced population transfer of R2. It is determined that the rise and decay times of these electron spin polarizations denote the spin−lattice relaxation time of the ground state and the lifetime of the excited multiplet state, respectively. This study contributes not only to an elucidation of radical−chromophore interactions but also to a novel approach for controlling magnetic properties by photoexcitation.

Introduction

Interactions between photoexcited triplet molecules and paramagnetic species result in some important phenomena, such as quenching of photoexcited molecules[1,2] and generation of the excited singlet oxygen.[3] Recently, a time-resolved electron paramagnetic resonance (TREPR) method, which is a powerful technique to observe paramagnetic intermediates after photoexcitation, has been proved to be useful for investigating the interactions between photoexcited triplet molecules and stable radicals. In the beginning, the radical-triplet pair mechanism (RTPM)[4] and the electron spin polarization transfer mechanism[5] have been reported for electron spin polarizations (ESPs) of the radicals, which are produced after the interaction with the excited triplet molecules. Further, some chromophores bonded to a paramagnetic molecule have been studied in order to achieve a direct investigation of excited multiplet states consisting of a photoexcited triplet chromophore and a doublet molecule.[6−8]

As a development of this kind of excited multiplet studies, new ESPs were reported for three-center four-spins (3c-4s) systems.[8b,9−11] The first is the photoinduced population transfer (PIPT) between the singlet (S_0') and triplet (T_0') ground states, observed for tetra-*tert*-butylphthalocyaninatosilicon (SiPc) co-

* To whom correspondence should be addressed.
[†] Department of Chemistry, Graduate School of Science.
[‡] Institute for Chemical Reaction Science.

(1) (a) Kuzmin, V. A.; Tatikolov, A. S.; Borisevich, Yu. E. *Chem. Phys. Lett.* **1978**, *53*, 52. (b) Kuzmin, V. A.; Tatikolov, A. S. *Chem. Phys. Lett.* **1978**, *53*, 606. (c) Watkins, A. R. *Chem. Phys. Lett.* **1980**, *70*, 262. (d) Schwerzel, R. E.; Caldwell, R. A. *J. Am. Chem. Soc.* **1973**, *95*, 1382. (e) Caldwell, R. A.; Schwerzel, R. E. *J. Am. Chem. Soc.* **1972**, *94*, 1035. (f) Chattopadhyay, S. K.; Das, P. K.; Hug, G. L. *J. Am. Chem. Soc.* **1983**, *105*, 6205. (g) Watkins, A. R. *Chem. Phys. Lett.* **1974**, *29*, 526. (h) Green, J. A., II; Singer, L. A.; Parks, J. H. *J. Chem. Phys.* **1973**, *58*, 2690. (i) Green, J. A., II; Singer, L. A. *J. Am. Chem. Soc.* **1974**, *96*, 2730.

(2) (a) Gouterman, M. In *The Porphyrins*; Dolphin, D., Ed.; Academic: New York, 1978; Vol. 3, pp 1−165. (b) Ferraudi, G. In *Phthalocyanines Properties and Applications*; Leznoff, C. C., Lever, A. B. P., Eds.; VCH Publishers: New York, 1989; Vol. I, pp 291−340.

(3) (a) Rosenthal, I.; Ben-Hur, E. In *Phthalocyanines Properties and Applications*; Leznoff, C. C., Lever, A. B. P., Eds.; VCH Publishers: New York, 1989; Vol. I, pp 393−425. (b) Rosenthal, I. In *Phthalocyanines Properties and Applications*; Leznoff, C. C., Lever, A. B. P., Eds.; VCH Publishers: New York, 1996; Vol. IV, pp 481−514 and many references therein.

(4) (a) Blättler, C.; Jent, F.; Paul, H. *Chem. Phys. Lett.* **1990**, *166*, 375. (b) Kawai, A.; Okutsu, T.; Obi, K. *J. Phys. Chem.* **1991**, *95*, 9130. (c) Kawai, A.; Obi, K. *J. Phys. Chem.* **1992**, *96*, 52. (d) Kawai, A.; Obi, K. *Res. Chem. Intermed.* **1993**, *19*, 865. (e) Turro, N. J.; Khudyakov, I. V.; Bossmann, S. H.; Dwyer, D. W. *J. Phys. Chem.* **1993**, *97*, 1138. (f) Jockusch, S.; Dedola, G.; Lem, G.; Turro, N. J. *J. Phys. Chem. B* **1999**, *103*, 9126. (g) Corvaja, C.; Franco, L.; Pasimeni, L.; Toffoletti, A.; Montanari, L. *Chem. Phys. Lett.* **1993**, *210*, 355. (h) Corvaja, C.; Franco, L.; Toffoletti, A. *Appl. Magn. Reson.* **1994**, *7*, 257. (i) Corvaja, C.; Franco, L.; Pasimeni, L.; Toffoletti, A. *J. Chem. Soc., Faraday Trans.* **1994**, *90*, 3267. (j) Hugerat, M.; van der Est, A.; Ojadi, E.; Biczok, L.; Linschitz, H.; Levanon, H.; Stehlik, D. *J. Phys. Chem.* **1996**, *100*, 495. (k) Regev, A.; Galili, T.; Levanon, H. *J. Phys. Chem.* **1996**, *100*, 18502.

(5) (a) Fujisawa, J.; Ishii, K.; Ohba, Y.; Iwaizumi, M.; Yamauchi, S. *J. Phys. Chem.* **1995**, *99*, 17082. (b) Fujisawa, J.; Ohba, Y.; Yamauchi, S. *J. Phys. Chem. A* **1997**, *101*, 434. (c) Jenks, W. S.; Turro, N. J. *Res. Chem. Intermed.* **1990**, *13*, 237.

(6) (a) Corvaja, C.; Maggini, M.; Prato, M.; Scorrano, G.; Venzin, M. *J. Am. Chem. Soc.* **1995**, *117*, 8857. (b) Corvaja, C.; Maggini, M.; Ruzzi, M.; Scorrano, G.; Toffoletti, A. *Appl. Magn. Reson.* **1997**, *12*, 477. (c) Mizuochi, N.; Ohba, Y.; Yamauchi, S. *J. Phys. Chem. A* **1997**, *101*, 5966. (d) Mizuochi, N.; Ohba, Y.; Yamauchi, S. *J. Chem. Phys.* **1999**, *111*, 3479.

10.1021/ja002780h CCC: $20.00 © 2001 American Chemical Society
Published on Web 01/03/2001

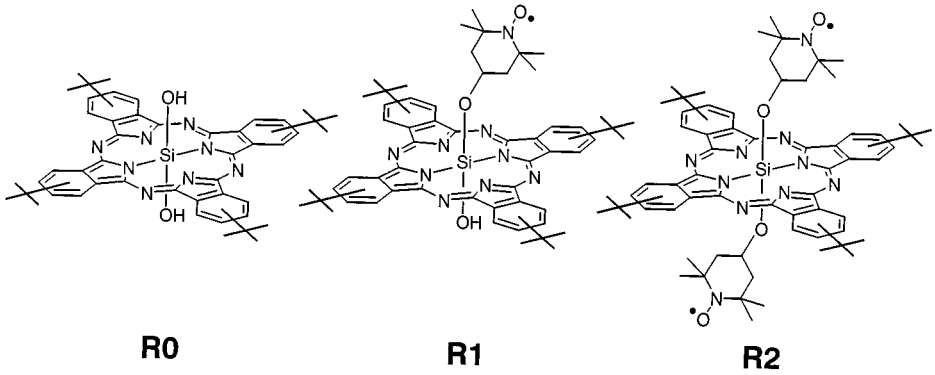

Figure 1. Molecular structures of R0, R1, and R2.

valently linked to two TEMPO radicals (R2 in Figure 1).[9] This PIPT results from selective population from the excited multiplet state to the T_0' state. The other is the radical-quartet pair mechanism (RQPM), observed for SiPc covalently linked to one TEMPO radical (R1 in Figure 1).[10] The RQPM is produced by an intermolecular interaction between R1 in the excited quartet state and another R1 in analogy with the RTPM. These ESPs are not only important for clarifying quenching of photoexcited molecules but also attractive as a new concept for controlling magnetic properties by light, because the magnetic properties in the ground state are varied before and after the photoexcitation. Since spin dynamics of these PIPT and RQPM had not been fully elucidated, more quantitative analyses are required.[9,10] Furthermore, it is important in the understanding of the influences of the linking radicals on photophysical properties to employ other spectroscopies, such as fluorescence or transient absorption, while there have been few studies on the chromophore bonded to stable radicals by using TREPR together with such optical measurements.

For these reasons, we present an investigation of R1 and R2 by the combined use of TREPR, fluorescence, and transient absorption spectroscopies. Important features are listed as follows. (1) The decay kinetics of SiPc in the lowest excited singlet and triplet states are investigated by fluorescence and transient absorption measurements. A relationship between intersystem crossing (ISC) and linking TEMPO radicals is discussed. (2) Since TREPR signals of both the excited multiplet state and the ground state are observable, the spin dynamics of the RQPM and PIPT are analyzed quantitatively not only by the signal of the excited multiplet state but also by the ESP of the ground state. The purpose of this work is to establish a novel approach for evaluating the excited-state dynamics of paramagnetic molecules.

Experimental Section

R0, R1, and R2 were synthesized following the methods already reported.[12] In particular, R1 and R2 were purified carefully before the measurements. Spectral grade toluene (Nacalai Tesque Inc.) was used as a solvent for all measurements. The concentrations of samples were $(0.2-1) \times 10^{-4}$ M for time-resolved fluorescence and transient absorption measurements, and 1×10^{-3} M for TREPR measurements. For these time-resolved measurements, samples were deaerated by freeze−pump−thaw cycles, and then the measurements were carried out within 2 days.

Steady-state UV−vis absorption spectra were measured with a Hitachi 330LC spectrometer. Steady-state fluorescence and excitation spectra were recorded with a Hitachi F-4500 fluorescence spectrometer. Fluorescence quantum yields were determined by the use of H_2Pc (= 0.60). Time-resolved fluorescence emissions were measured by a single-photon counting method using an argon ion laser (Spectra-Physics, BeamLok 2060-10-SA), a pumped Ti:sapphire laser (Spectra-Physics, Tsunami 3950-L2S, 1.5 ps fwhm) with a pulse selector (Spectra-Physics, Model 3980), a second harmonic generator (GWU-23PS), and a streak-scope (Hamamatsu Photonics, C4334-01).[13] For the time-resolved fluorescence measurements, samples were excited at 365 nm. Transient absorption measurements were performed by using a monochromator (JASCO CT-25CP) and a photomultiplier (Hamamatsu Photonics R446) with a continuous wave of metal halide lamp (Sigma Koki IMH-250). TREPR, pulse-EPR, and steady-state EPR measurements were carried out on a Bruker ESP 300E spectrometer.[10,14] For the transient absorption and TREPR measurements, samples were excited at 620 or 585 nm by a dye laser (Lumonics HD 500) pumped with an excimer laser (Lumonics EX 500, 13 ns fwhm), and the signals were integrated using a digital oscilloscope (Iwatsu-LeCroy LT342). All experiments were made at room temperature.

Theoretical Background

To discuss the electron spin dynamics, the excited states of R0, R1, and R2 are illustrated. Simple energy diagrams of the excited states are shown in Figure 2. For R0, the lowest excited singlet (S_1) state is almost derived from the $^1(a_{1u}e_g)$ configuration (the a_{1u} (π) and e_g (π^*) orbitals denote the HOMO and LUMO of Pc ligand, respectively), and is located at ~14500 cm^{-1}.[12] The lowest excited triplet (T_1) state also originates from the $^3(a_{1u}e_g)$ configuration, and is located at ~9000 cm^{-1}.[15]

For R1, the doublet ground (D_0) state consists of TEMPO in the D_0 state (^{2}TEMPO) and SiPc in the singlet ground (S_0) state (^{1}SiPc). A pair of ^{2}TEMPO and SiPc in the S_1 state (^{1}SiPc*) provides the excited doublet (D_n) state. On the other hand, the lowest excited doublet (D_1) and quartet (QA_1) states are

(7) (a) Ishii, K.; Fujisawa, J.; Ohba, Y.; Yamauchi, S. *J. Am. Chem. Soc.* **1996**, *118*, 13079. (b) Fujisawa, J.; Ishii, K.; Ohba, Y.; Yamauchi, S.; Fuhs, M.; Möbius, K. *J. Phys. Chem. A* **1997**, *101*, 5869. (c) Ishii, K.; Fujisawa, J.; Adachi, A.; Yamauchi, S.; Kobayashi, N. *J. Am. Chem. Soc.* **1998**, *120*, 3152. (d) Fujisawa, J.; Ishii, K.; Ohba, Y.; Yamauchi, S.; Fuhs, M.; Möbius, K. *J. Phys. Chem. A* **1999**, *103*, 213. (e) Ishii, K.; Ishizaki, T.; Kobayashi, N. *J. Phys. Chem. A* **1999**, *103*, 6060. (f) Ishii, K.; Kobayashi, N. *Coord. Chem. Rev.* **2000**, *198*, 231.

(8) Very recently, the excited multiplet studies have been reported for novel systems. (a) Asano-Someda, M.; van der Est, A.; Krüger, U.; Stehlik, D.; Kaizu, Y.; Levanon, H. *J. Phys. Chem. A* **1999**, *103*, 6704. (b) Teki, Y.; Miyamoto, S.; Iimura, K.; Nakatsuji, M.; Miura, Y. *J. Am. Chem. Soc.* **2000**, *122*, 984.

(9) Ishii, K.; Hirose, Y.; Kobayashi, N. *J. Am. Chem. Soc.* **1998**, *120*, 10551.

(10) Ishii, K.; Hirose, Y.; Kobayashi, N. *J. Phys. Chem. A* **1999**, *103*, 1986.

(11) Mizuochi, N.; Ohba, Y.; Yamauchi, S. *J. Phys. Chem. A* **1999**, *103*, 7749.

(12) Ishii, K.; Hirose, Y.; Kobayashi, N. *J. Porphyrins Phthalocyanines* **1999**, *3*, 439.

(13) Fujitsuka, M.; Sato, T.; Shimidzu, T.; Watanabe, A.; Ito, O. *J. Phys. Chem. A* **1997**, *101*, 1056.

(14) Fukuju, T.; Yashiro, H.; Maeda, K.; Murai, H. *Chem. Phys. Lett.* **1999**, *304*, 173.

(15) Vincett, P. S.; Voigt, E. M.; Rieckoff, K. E. *J. Chem. Phys.* **1971**, *55*, 4131.

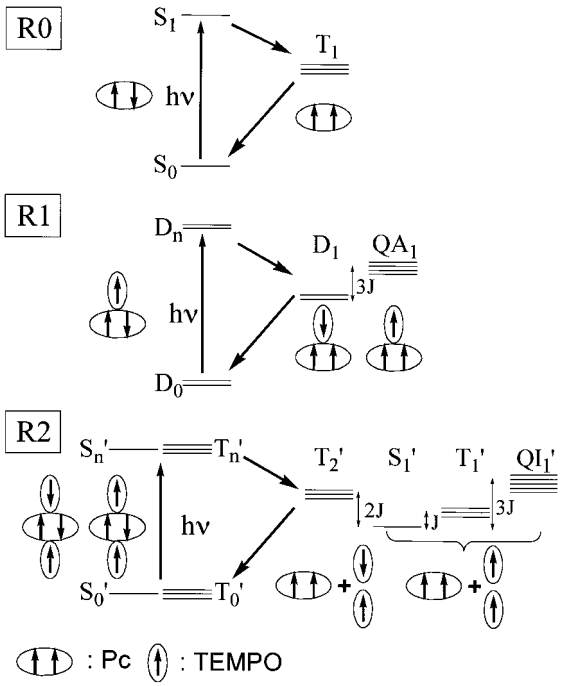

Figure 2. Energy diagrams of the excited states of R0, R1, and R2. The *J* value is assumed to be negative in these diagrams.

generated by an interaction between ^{2}TEMPO and SiPc in the T_1 state (^{3}SiPc*).[16] Previous TREPR studies indicate that an energy splitting ($3J$) between the D_1 and QA_1 states is evaluated as > 0.1 cm^{-1}.[10,17]

In case of R2, the singlet (S_0') and triplet (T_0') ground states are generated by an interaction between two ^{2}TEMPO radicals. An energy splitting ($2J'$) between the S_0' and T_0' states is evaluated as 9.9×10^{-4} cm^{-1} by a steady-state EPR spectrum.[9] The excited singlet (S_n') and triplet (T_n') states are constituted by ^{1}SiPc* and two ^{2}TEMPO. On the other hand, interactions with ^{3}SiPc* (3c-4s system) are complicated. The interactions among ^{3}SiPc* and two ^{2}TEMPO result in the lowest excited singlet (S_1'), triplet (T_1'), quintet (QI_1'), and second lowest excited triplet (T_2') states.[16] Here, two ^{2}TEMPO radicals exhibit the triplet and singlet characters in the T_1' and T_2' states, respectively. Energies of the S_1', T_1', T_2', and QI_1' states are calculated as $J - J'$, $-J'$, $-J$, and $-2J - J'$, respectively.[16b] Since J ($>3.3 \times 10^{-2}$ cm^{-1}) $\gg J'$ ($\sim 5 \times 10^{-4}$ cm^{-1}), they are reevaluated as J, 0, $-J$, $-2J$, respectively.

Results and Interpretations

Fluorescence and Transient Absorption Measurements. Steady-state electronic absorption and fluorescence spectra of R1 are shown in Figure 3. Electronic absorption spectra show little dependence on substitution of TEMPO radicals, indicating that the electronic interaction between the excited singlet SiPc and doublet TEMPO is very weak.[12] While the fluorescence spectra are also independent of the TEMPO substitution, the fluorescence quantum yield decreases in the order R0 (= 0.57), R1 (= 0.21), and R2 (= 0.012).[12] To investigate in detail, time-resolved fluorescence emissions of R0, R1, and R2 were measured. Decay-profiles of fluorescence are shown in Figure 4, and the lifetimes are summarized in Table 1. The decay-

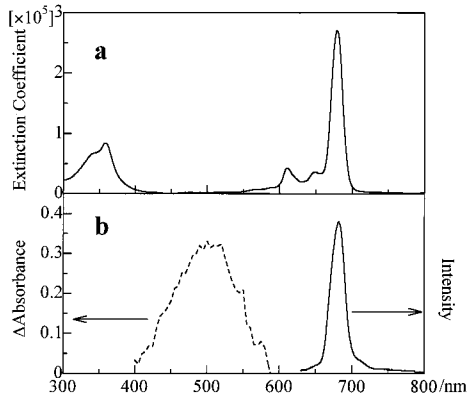

Figure 3. Steady-state electronic absorption (**a**), fluorescence (**b**; solid line), and transient absorption (**b**; broken line) spectra of R1. The transient absorption spectrum was observed at 2.2 μs after 620 nm laser excitation.

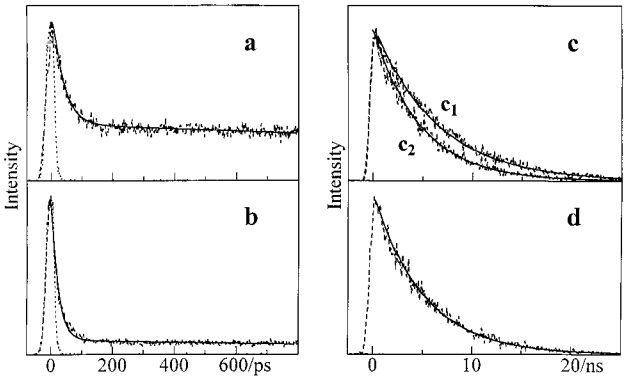

Figure 4. Decay-profiles of fluorescence (broken lines) of R1 (**a**, $\mathbf{c_2}$), R2 (**b, d**), and R0 ($\mathbf{c_1}$) with their fitting curves (solid lines). Time-profiles of laser pulses are shown by dotted lines (**a**, **b**). Fitting curves were calculated by a least-squares method.

profile of R0 was analyzed with a single-exponential function, where the lifetime (= 6.8 ns) is similar to those of metal-free or Mg Pc derivatives.[18] On the other hand, the fluorescence decays of R1 and R2 are faster than that of R0, and consist of fast and slow components, whose decay times were evaluated as several 10 picoseconds (R1 = 42 ps, R2 < 30 ps) and several nanoseconds (R1 = 4.7 ns, R2 = 4.7 ns), respectively. Since time-resolved fluorescence spectra of the fast and slow components are similar to the steady-state fluorescence spectra, it is confirmed that both the fast and slow fluorescence emissions originate from ^{1}SiPc*.[19] To investigate ^{3}SiPc*, transient absorption measurements were carried out for R0, R1, and R2. A transient absorption spectrum of R1 is typically shown in Figure 3b. Transient absorption spectra of all complexes exhibit typical T−T absorption spectra of Pc derivatives,[20] indicating that the electronic interaction between the excited triplet SiPc and doublet TEMPO is small. Decay-profiles of the transient absorption signals are shown in Figure 5. The decay-profiles of R0 are remarkably dependent on the laser power, originating from T−T annihilation.[21] In contrast, the decay-profiles of R1

(16) (a) Bencini, A.; Gatteschi, D. *EPR of Exchange Coupled Systems*; Springer-Verlag: Berlin, 1990. (b) Kahn, O. *Molecular Magnetism*; Wiley−VCH: New York, 1993.

(17) Ishii, K.; Ishizaki, T.; Kobayashi, N. *Inorg. Chem.* Manuscript submitted.

(18) (a) Ohtani, H.; Kobayashi, T.; Ohno, T.; Kato, S.; Tanno, T.; Yamada, A. *J. Phys. Chem.* **1984**, *88*, 4431. (b) Kaneko, Y.; Nishimura, Y.; Takane, N.; Arai, T.; Sakuragi, H.; Kobayashi, N.; Matsunaga, D.; Pac, C.; Tokumaru, K. *J. Photochem. Photobiol. A* **1997**, *106*, 177.

(19) The fluorescence decays were independent of the concentration [$(0.2-1) \times 10^{-4}$ M], indicating that an intermolecular process is not important.

(20) (a) Ferencz, A.; Neher, D.; Schulze, M.; Wegner, G.; Viaene, L.; De Schryver, F. C. *Chem. Phys. Lett.* **1995**, *245*, 23. (b) Fernández, D. A.; Awruch, J.; Dicelio, L. E. *Photochem. Photobiol.* **1996**, *63*, 784.

Table 1. Lifetimes of ^{1}SiPc* and ^{3}SiPc*

observed signals	R0	R1	R2
fluorescence ^{1}SiPc*	6.8 ± 0.4 ns	42 ± 4 ps(~75%) 4.7 ± 0.3 ns(~25%)	<30 ps(~90%) 4.7 ± 0.3 ns(~ 10%)
transient absorption ^{3}SiPc*	500 ± 30 μs	7.6 ± 0.3 μs	3.7 ± 0.4 μs
TREPR (excited state) ^{3}SiPc*	–	5.1 ± 0.9 μs	–
TREPR (ground state) ^{3}SiPc*	–	5.5 ± 0.6 μs	1.8 ± 0.2 μs

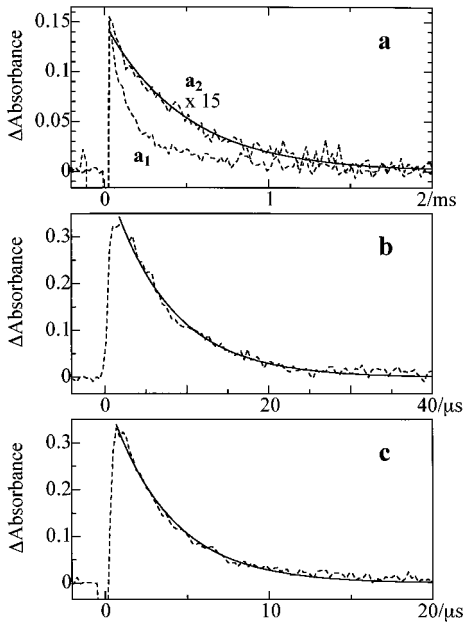

Figure 5. Decay-profiles of transient absorption signals (broken lines) of R0 ($\mathbf{a_1}$, $\mathbf{a_2}$), R1 (**b**), and R2 (**c**) at 490 nm with their fitting curves (solid lines). For R0, two decay-profiles measured using strong ($\mathbf{a_1}$; 5.8 mJ/pulse) and weak ($\mathbf{a_2}$; ~0.1 mJ/pulse) laser excitation are shown. Fitting curves were calculated by a least-squares method.

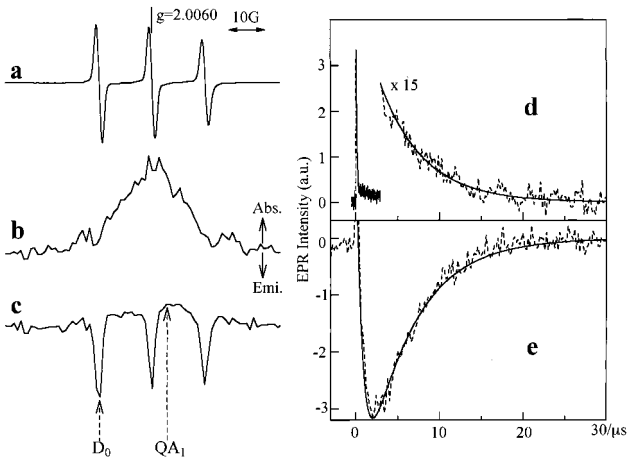

Figure 6. A steady-state EPR spectrum (**a**), TREPR spectra (**b**, **c**), and time-profiles of the QA_1 and D_0 signals (**d**, **e**; broken lines) of R1 with their fitting curves (**d**, **e**; solid lines). TREPR spectra were observed at 0.1 (**b**) and 3.6 (**c**) μs after 585 nm laser excitation. Time-profiles of the QA_1 and D_0 signals were measured at positions indicated by the QA_1 and D_0 arrows, respectively. Fitting curves were calculated by a least-squares method.

and R2 were independent of the laser power, indicating that the intramolecular quenching is more efficient than the intermolecular quenching. The decay-profiles, except for R0 with the strong laser excitation, were analyzed with single-exponential functions. The lifetimes of R0, R1, and R2 were evaluated as 500 μs, 7.6 μs, and 3.7 μs (Table 1), respectively, and are markedly dependent on the number of TEMPO radicals.

TREPR Measurements. Steady-state EPR and TREPR spectra of R1 are shown in Figure 6a, b, and c. A broad *A* signal of the QA_1 R1 is seen at 0.1 μs after laser excitation,[10] and is generated by selective ISC from the higher excited doublet states. Here, *A* and *E* denote absorption and emission of the microwaves, respectively. In contrast, the *E* polarization is generated in the D_0 state, and is reasonably assigned to the RQPM,[10] where the excess α spin is produced by the intermolecular interaction between the QA_1 R1 and another R1. To discuss quantitatively, time-profiles of the TREPR signals were measured, and are shown in Figure 6d and e.[22] For the QA_1 signal, the time-profile of the *A* signal was analyzed with a double-exponential function ($\tau_1 < 0.1$ μs and $\tau_2 = 5.1 \pm 0.9$ μs). The fast and slow decay times are reasonably assigned to the spin−lattice relaxation (SLR) time and lifetime of the QA_1 state, respectively. The QA_1 lifetime measured by TREPR is a little different from that observed by the transient absorption measurement. This originates from a change in experimental conditions, such as concentration or magnetic field.[23] On the other hand, the rise and decay times of the *E* polarization in the D_0 state were evaluated as 0.71 ± 0.04 and 5.5 ± 0.6 μs, respectively.

A steady-state EPR spectrum of R2 is shown in Figure 7a.[9] The spectrum is conveniently divided into two groups. One is κ_n signals ($n = 1-3$), which are transitions when $m_{N1} = m_{N2}$, where the m_{Ni} ($i = 1, 2$) is the magnetic quantum number of the nitrogen nucleus *i*. The eigenfunctions are represented as $|T_{0+}'\rangle$, $|T_{00}'\rangle$, $|S_0'\rangle$, and $|T_{0-}'\rangle$ without the S − T_0 mixing.[24] The other is σ_n and η_n signals, which are transitions when $m_{N1} \neq m_{N2}$. The eigenfunctions are $|T_{0+}'\rangle$, $|T_{0-}'\rangle$, $|\psi_1'\rangle$ (= $a|S_0'\rangle + b|T_{00}'\rangle$), and $|\psi_2'\rangle$ (= $-b|S_0'\rangle + a|T_{00}'\rangle$) with the S−$T_0$ mixing. TREPR spectra of R2 are shown in Figure 7b, c, and d.[9] A broad *E* signal ($g = 2.003$) is seen at 0.1 μs after laser excitation. This signal is evidently different from the ground state and is reasonably assigned to the excited multiplet state.[25] The excited multiplet state of the 3c-4s system was observed in solution

(21) Frink, M. E.; Geiger, D. K.; Ferraudi, G. J. *J. Phys. Chem.* **1986**, *90*, 1924.

(22) The time-profiles of TREPR signals were independent of the microwave power (0.05−5 mW).

(23) While TREPR measurements were carried out for [R1] = 1×10^{-4} M, significant time-profiles could not be obtained.

(24) $|T_{0+}'\rangle = |\alpha\alpha\rangle$, $|T_{00}'\rangle = (|\alpha\beta\rangle + |\beta\alpha\rangle)/2^{1/2}$, $|S_0'\rangle = (|\alpha\beta\rangle - |\beta\alpha\rangle)/2^{1/2}$, $|T_{0-}'\rangle = |\beta\beta\rangle$.

(25) *g* Values of the T_1', T_2', and QI_1' states were calculated as 2.003, 2.000, and 2.003, respectively, by using $g(T_2') = g(T)$ and $g(T_1') = g(QI_1') = \{g(T) + g(R)\}/2$,[16] where $g(T)$ (= 2.000) and $g(R)$ (= 2.006) denote the *g* values of ^{3}SiPc* and ^{2}TEMPO, respectively. While the $g(QI_1')$ and $g(T_1')$ values are the same as the *g* value (= 2.003) of the broad *E* signal, it is difficult to assign the broad *E* signal clearly due to the small energy splitting (~*J*) and the complicated TREPR spectrum of R2 at 20 K.[7f]

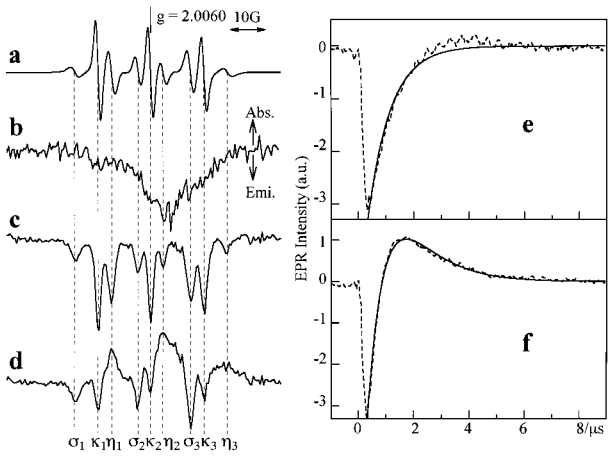

Figure 7. A steady-state EPR spectrum (**a**), TREPR spectra (**b**, **c**, **d**) and time-profiles of the κ_2 and η_2 signals (**e**, **f**; broken lines) of R2 with their fitting curves (**e**, **f**; solid lines). TREPR spectra were observed at 0.1 (**b**), 0.6 (**c**), and 1.8 (**d**) μs after 585 nm laser excitation. Fitting curves were calculated by a least-squares method.

for the first time. The *EEE EEE EEE* and *EEA EEA EEA* signals of the ground state are seen at 0.6 and 1.8 μs, respectively. The first *EEE EEE EEE* polarizations originate from the excess α spin generated in the excited multiplet state. The later *EEA EEA EEA* polarizations are interpreted by selective population to the T_0' state, since the decays from the T_1', T_2', and QI_1' states to the T_0' state are faster than those to the S_0' state for the smaller change in the spin quantum number. To investigate the spin dynamics in detail, time-profiles of the TREPR signals were measured, and are typically shown in Figure 7e and f. The decay-profile of the κ_2 signal was analyzed with a single-exponential function, where the decay time (0.72 ± 0.1 μs) is almost the same as the SLR time (0.71 ± 0.03 μs) measured by the inversion recovery method.[26] This analysis indicates that the ESP of the κ_n signal is initially generated by a transfer of the excess α spin from the excited multiplet state to the ground state, and is not produced after that. On the other hand, the time-profile of the η_2 signal is different from that of the κ_2 signal. After the decay of the first *E* polarization, a new *A* polarization is generated. The time-profile of the η_2 signal was analyzed with a double-exponential function ($\tau_1 = 0.55 \pm 0.12$ μs and $\tau_2 = 1.8 \pm 0.2$ μs).

Discussion

Fluorescence and Transient Absorption. It is found that the fluorescence quantum yields and lifetimes of R1 and R2 remarkably decrease compared with those of R0. These changes in fluorescence properties are reasonably interpreted by the interaction with ^{2}TEMPO, which changes ISC between the singlet and triplet states to spin-allowed transitions, such as, $D_n \rightarrow D_1$, $S_n' \rightarrow S_1'$, $T_n' \rightarrow T_1'$, or $T_n' \rightarrow T_2'$. The fluorescence decays of R1 and R2 consist of fast (several 10 ps) and slow (~5 ns) components in contrast to the single-exponential decay of R0. These fluorescence decay behaviors remain to be fully explored but may be interpreted by a change in the relative geometry between SiPc and flexible axial ligands,[27] providing both large and small interactions between TEMPO and SiPc in a time-resolved fluorescence time-scale.

Scheme 1

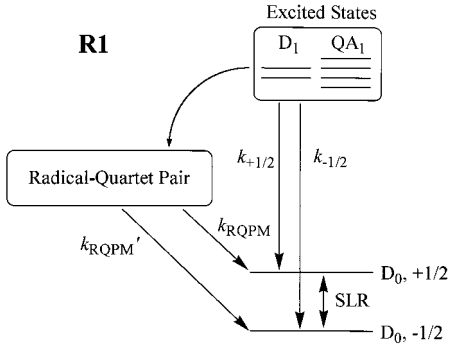

All decay-profiles of the transient absorption signals are analyzed with single-exponential functions. The lifetime decreases in the order R0 (= 500 μs), R1 (= 7.6 μs), and R2 (= 3.7 μs), and is markedly dependent on the number of TEMPO radicals. From here, an origin of these short lifetimes is considered. For R1, only the QA_1 state could be observed by TREPR measurements in contrast to no D_1 signal.[10] However, the short lifetime of R1 needs a contribution of the D_1 state, since a transition between the QA_1 and D_0 states is spin-forbidden.[28] In this case, differential equations are expressed as follows.

$$d[QA_1]/dt = -(k_1 + k_{-3})[QA_1] + k_3[D_1] \quad (1a)$$

$$d[D_1]/dt = -(k_2 + k_3)[D_1] + k_{-3}[QA_1] \quad (1b)$$

Here, k_1, k_2, k_3, and k_{-3} denote the rate constants of the $QA_1 \rightarrow D_0$, $D_1 \rightarrow D_0$, $D_1 \rightarrow QA_1$, and $QA_1 \rightarrow D_1$ transitions, respectively. While an analytical solution of eq 1 is a double-exponential function, the decay of the transient absorption signal becomes a single-exponential function due to the rapid averaging between the D_1 and QA_1 states (k_3, $k_{-3} \gg k_1$, k_2).[29] Assuming $3J \ll kT$, the decay rate of the transient absorption signal is given by $(2k_1 + k_2)/3$. When $k_2 \gg k_1$,[28] the k_2 value was calculated as 3.9×10^5 s^{-1}. In a similar manner, the decay rate of R2 is given by $(k_4 + k_5 + 3k_6 + 3k_7 + 3k_8 + 3k_9 + 5k_{10} + 5k_{11})/12$, where k_4, k_5, k_6, k_7, k_8, k_9, k_{10}, k_{11} denote the decay rate constants of the $S_1' \rightarrow S_0'$, $S_1' \rightarrow T_0'$, $T_1' \rightarrow S_0'$, $T_1' \rightarrow T_0'$, $T_2' \rightarrow S_0'$, $T_2' \rightarrow T_0'$, $QI_1' \rightarrow S_0'$, and $QI_1' \rightarrow T_0'$ transitions, respectively. When the rate constants (k_5, k_6, k_8, k_{10}, and k_{11}) of spin-forbidden transitions are negligibly small,[28] the rate constants (k_4, k_7, and k_9) of spin-allowed transitions were estimated as 4.6×10^5 s^{-1}, and are a little larger than the k_2 value ($= 3.9 \times 10^5$ s^{-1}). In conclusion, the short lifetimes of R1 and R2 originate from a contribution of the spin-allowed transitions.

TREPR of R1. The time-profile of the *E* polarization in the D_0 state is analyzed with a double-exponential function ($\tau_1 = 0.71$ μs and $\tau_2 = 5.5$ μs). To discuss quantitatively, the spin dynamics of the RQPM were investigated using following differential equations (Scheme 1).

$$d[D_0 + {}^1/_2]/dt = k_{+1/2}\{[QA_1] + [D_1]\} + k_{RQPM}[QA_1][R1] + (N - N_B)/(2T_{1SLR}) \quad (2a)$$

(26) The inversion recovery method was carried out using a $\pi - \pi/2$ pulse sequence.

(27) An exchange between stable conformations in the excited state or a difference in the most stable conformation between the ground and excited states are considered as possible origins.

(28) Since the similarity of the wave functions indicates that the decay rate of the QA_1 R1 is almost the same as that ($= 2 \times 10^3$ s^{-1}) of the T_1 R0,[7e] the decay rate of the spin-allowed transitions is much faster than that of the spin-forbidden transitions.

(29) Asano, M.; Kaizu, Y.; Kobayashi, H. *J. Chem. Phys.* **1988**, *89*, 6567.

$$d[D_0 - {}^1/_2]/dt = k_{-1/2}\{[QA_1] + [D_1]\} + k_{RQPM}'[QA_1][R1] - (N - N_B)/(2T_{1SLR}) \quad (2b)$$

$$N = [D_0 - {}^1/_2] - [D_0 + {}^1/_2] \quad (2c)$$

$$N_B = [D_0 - {}^1/_2]_B - [D_0 + {}^1/_2]_B \quad (2d)$$

Here, N_B, T_{1SLR}, and $1/(k_{+1/2} + k_{-1/2})$ denote the Boltzmann difference, SLR time of the D_0 state, and lifetime of the D_1 and QA_1 states without the RQPM, respectively. We assume that the interaction between the QA_1 R1 and another R1 results in the RQPM, and that k_{RQPM} and k_{RQPM}' are independent of the ESP in the QA_1 and D_0 states. After the SLR in the QA_1 state, the decay of the QA_1 state is expressed as

$$[QA_1] = [QA_1]_0 \exp(-k_M t) \quad (3)$$

Here, $1/k_M$ and $[QA_1]_0$ denote the lifetime of the QA_1 state with the RQPM and the initial concentration of the QA_1 state after laser excitation, respectively. Assuming $k_{+1/2} = k_{-1/2}$, the differential equation and analytical solution of the *E* polarization are expressed as follows:

$$dN/dt = (k_{RQPM}' - k_{RQPM})\,[QA_1]_0[R1] \exp(-k_M t) - (1/T_{1SLR})(N - N_B) \quad (4a)$$

$$N = \{(k_{RQPM}' - k_{RQPM})[QA_1]_0[R1]/(1/T_{1SLR} - k_M)\} \times \{\exp(-k_M t) - \exp(-t/T_{1SLR})\} + N_B \quad (4b)$$

The analytical solution is expressed by a double-exponential function, where the rising and decaying parts indicate the SLR time ($= T_{1SLR}$) of the D_0 state and the lifetime ($= 1/k_M$) of the QA_1 state, respectively. The fast rise time ($= 0.71$ μs) of the *E* polarization is almost similar to the SLR time ($= 0.67 \pm 0.07$ μs) measured by the inversion recovery method.[26] In addition, the decay time ($= 5.5$ μs) of the *E* polarization approximates to the lifetime ($= 5.1$ μs) of the QA_1 state measured by TREPR. That is, the RQPM is well reproduced by eq 4b. The spin dynamics of R1 are summarized in Figure 8. The excess β spin in the QA_1 state is generated by selective ISC promoted by the SOC. The *A* polarization of the QA_1 state decays with the SLR time (<0.1 μs) of the QA_1 state. After the SLR, the QA_1 R1 in the Boltzmann distribution interacts with another R1, resulting in the *E* polarization. The *E* polarization rises with the SLR time ($= 0.7$ μs) of the D_0 state, and decays with the lifetime ($= 5.5$ μs) of the QA_1 state.

TREPR of R2. The *E* polarization decay at the κ_2 position is analyzed with a single-exponential function, whose decay time ($= 0.72$ μs) is the same as the SLR time ($= 0.71$ μs). This indicates that the ESP of the κ_n transitions is not produced after the transfer of the excess α spin from the excited multiplet state.

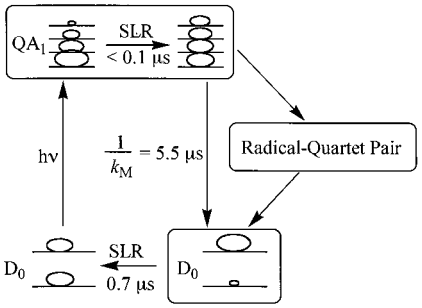

Figure 8. Summary of spin-dynamics of R1 after laser excitation.

Scheme 2

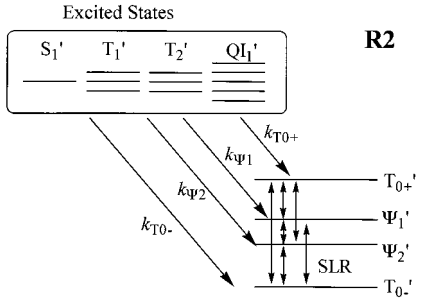

On the other hand, the time-profile of the η_2 signal is different from that of the κ_2 signal. After the decay of the initial *E* polarization, the new *A* polarization is generated by selective population to the T_0' state. Using Scheme 2, a differential equation of the η_2 signal is expressed as follows:

$$dN'/dt = (k_{T0-} - k_{\Psi i})\,[M'] - (1/T_{1SLR}')(N' - N_B') \quad (5a)$$

$$[M'] = [S_1'] + [T_1'] + [T_2'] + [QI_1'] \quad (5b)$$

$$N' = [T_{0-}'] - [\Psi_i'] \quad (5c)$$

$$N_B' = [T_{0-}']_B - [\Psi_i']_B \quad (5d)$$

$$i = 1, 2$$

After the SLR in the excited multiplet state, the time-profile of the excited multiplet state is expressed as

$$[M'] = [M']_0 \exp(-k_M' t) \quad (6)$$

Here, $1/k_M'$ and $[M']_0$ denote the lifetime and initial concentration of the excited multiplet state, respectively. Using eq 6, an analytical solution of eq 5a is expressed by a double-exponential function.

$$N' = \{(k_{T0-} - k_{\Psi i})\,[M']_0/(1/T_{1SLR}' - k_M')\} \times \{\exp(-k_M' t) - (1 - P)\exp(-t/T_{1SLR}')\} + N_B' \quad (7a)$$

$$P = (1/T_{1SLR}' - k_M')(N_0' - N_B')/\{(k_{T0-} - k_{\Psi i})[M']_0\} \quad (7b)$$

$$N_0' = [T_{0-}']_0 - [\Psi_i']_0 \quad (7c)$$

Here, N_0' denotes the initial *E* polarization transferred from the excited multiplet state. That is, the rising and decaying parts of the η_2 signal exhibit the SLR time of the ground state and the lifetime of the excited multiplet state, respectively. The rise time ($= 0.55 \pm 0.12$ μs) of the *A* polarization approximates to the SLR time ($= 0.71 \pm 0.03$ μs) of the ground state. While the decay time ($= 1.8$ μs) of the *A* polarization is shorter than the lifetime ($= 3.7$ μs) of the excited multiplet state measured by transient absorption, this is due to the change in experimental conditions, concentration or magnetic field. Therefore, the spin dynamics of the PIPT phenomenon are reasonably explained by eq 7, and are summarized in Figure 9. The excess α spin in the excited multiplet state is generated by selective ISC. The *E* polarization of the excited multiplet state is transferred to the ground state, and decays with the SLR time (<0.1 μs) of the excited multiplet state. After the SLR, selective population from the excited multiplet state occurs to the T_0' state. The *A* polarization of the η_n signals rises with the SLR time ($= 0.7$

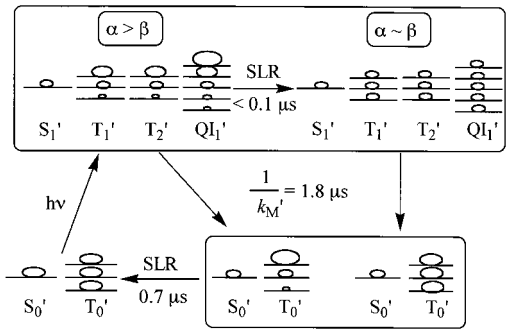

Figure 9. Summary of spin-dynamics of R2 after laser excitation.

μs) of the ground state, and decays with the lifetime (= 1.8 μs) of the excited multiplet state.

Conclusions

We have studied SiPc covalently linked to one or two TEMPO radicals, R1 and R2, and succeeded in clarifying the photophysical properties by the combined use of fluorescence, transient absorption, and TREPR spectroscopies. The decay kinetics of ^{1}SiPc* and ^{3}SiPc* were investigated by the fluorescence and transient absorption measurements, and was explained by the interaction with ^{2}TEMPO changing the ISC between ^{3}SiPc* and ^{1}SiPc* or ^{1}SiPc to spin-allowed transitions. Quantitative analyses of the PIPT and RQPM showed that the rise and decay times of these ESPs were the SLR time of the ground state and the lifetime of the excited multiplet state, respectively. This study contributes not only to an elucidation of radical-chromophore interactions, but also to a novel approach for controlling magnetic properties by photoexcitation.

Acknowledgment. This work was partially carried out in the Advanced Instrumental Laboratory for Graduate Research of the Department of Chemistry, Graduate School of Science, Tohoku University, and was supported by a Grant-in-Aid for Scientific Research (B) No. 11440192 and for Encouragement of Young Scientists No. 12740355 from the Ministry of Education, Science, Sports, and Culture, Japan, and by the Asahi Glass Foundation.

JA002780H